Available online at www.sciencedirect.com
ScienceDirect
Journal of Catalysis 248 (2007) 46–52
JOURNAL OF CATALYSIS
www.elsevier.com/locate/jcat

Large-capacity oxygen storage of Pd-loaded $Pr_2O_2SO_4$ applied to anaerobic catalytic CO oxidation

Keita Ikeue, Masakazu Eto, Dong-Jie Zhang, Tomoatsu Kawano, Masato Machida *

Department of Nano Science and Technology, Graduate School of Science and Engineering, Kumamoto University, 2-39-1 Kurokami, Kumamoto 860-8555, Japan

Received 22 January 2007; revised 6 March 2007; accepted 6 March 2007

Abstract

The oxygen release and storage properties of 1 wt% Pd-loaded $Pr_2O_2SO_4$ were studied using different cycled feed stream methods, namely a flow microbalance, in situ X-ray diffraction and anaerobic CO oxidation in a flow reactor. The redox between $Pr_2O_2SO_4$ and Pr_2O_2S exhibited a large oxygen storage of 2 (mol of O_2) mol^{-1} at high temperatures. Loading Pd can activate reducing gases (H_2/CO) so as to promote the oxygen release by the reduction of bulk $Pr_2O_2SO_4$ to Pr_2O_2S. In contrast, the oxygen storage by the reoxidation of Pr_2O_2S to $Pr_2O_2SO_4$ was much faster even in the absence of Pd, because the redox between Pr^{3+} and Pr^{4+} on the solid surface plays the role of a mediator. Pd species also formed active catalytic sites for an anaerobic CO oxidation, which consumed lattice oxygens released from $Pr_2O_2SO_4$. The full capacity oxygen storage of 2 (mol of O_2) mol^{-1} and anaerobic oxidation of 4 (mol of CO) mol^{-1} could be cycled. The CO/O_2 cycled feed stream reactions achieved CO conversion >85% at 700 °C, almost comparable to that of a steady-state CO-O_2 reaction. The catalytic activity was not affected by the presence of SO_2, which rather improved the stability of $Pr_2O_2SO_4$/Pr_2O_2S.

Keywords: Oxygen storage; Oxysulfate; Praseodymium; Anaerobic oxidation

1. Introduction

Oxygen storage materials have become important in applications to an automotive emission control catalyst to compensate for the oscillation between lean and rich exhaust conditions that change momentarily [1–3]. This is very important for the present three-way catalyst to achieve efficient conversions of NO_x, CO, and hydrocarbons under stoichiometric conditions. The most widely used material for this purpose is CeO_2-ZrO_2 [4–10] because of the fast and reversible redox reaction, $CeO_2 \rightleftarrows CeO_{2-x} + (x/2)O_2$, and thermal and chemical stabilities. The most noticeable feature of this material is very quick release and storage of oxygen in response to the oxygen partial pressure in the gas phase, the oxygen storage capacity (OSC) of which cannot exceed 0.25 (mol of O_2) mol^{-1}. In contrast, we have recently discovered that the redox between $Ln_2O_2SO_4$ (S^{6+}) and Ln_2O_2S (S^{2-}) achieved the OSC of 2 (mol of O_2) mol^{-1} [11,12], which is eight times larger than that of CeO_2-ZrO_2. It should be noted that this is the first successful oxygen storage that uses the nonmetallic element (S) as a redox site instead of metallic cations. Although the reversible redox cycles of thermostable $Ln_2O_2SO_4$ with Ln = La, Sm, and Nd are possible only at high temperatures (above 700 °C), the Pr system can work at an exceptionally low temperature (600 °C). The smooth reduction of $Pr_2O_2SO_4$ is associated with the structural distortion of an SO_4^{2-} unit, and reoxidation is promoted by the easy redox of Pr^{3+}/Pr^{4+} on the surface of Pr_2O_2S [13]. The redox of the Pr system can further be accelerated in the presence of an impregnated noble metal, such as 1 wt% Pd or Pt. The microstructural modification by means of template synthesis also increases the specific surface area and thus the rate of oxygen storage and release [14]. In previous work, we developed Pr oxysulfate with large and fast oxygen storage.

To apply this large OSC material for the conversion of noxious gases in the exhaust, the catalyst design of noble metal

* Corresponding author. Fax: +81 96 342 3651.
E-mail address: machida@chem.kumamoto-u.ac.jp (M. Machida).

0021-9517/$ – see front matter
doi:10.1016/j.jcat.2007.03.003

catalyst-loaded oxysulfates is needed. As a number of studies on CeO_2-ZrO_2 have noted, the total (maximum) OSC is not always a measure of automobile catalytic performance in oscillating lean/rich cycles occurring with a frequency of about 1 Hz [15–18]. This is because the amount of oxygen transferred in such a short transient process becomes more important than the total capacity of oxygen that can be removed. Nevertheless, the large OSC is useful in cases where the catalyst may be exposed to lean or rich exhausts for a longer time or with a larger deviation from the stoichiometric A/F ratio. In addition, new materials with a larger OSC may open up new applications of oxygen storage besides automotive catalysts. For catalytic applications, metal catalysts are needed to facilitate full-capacity oxygen release as well as the most rapid storage possible at a given temperature. According to our previous work [12,13], the total OSC of 1 wt% Pd/$Pr_2O_2SO_4$ measured using a flow microbalance under low-frequency H_2/O_2 cycled feed stream conditions was consistent with the ideal OSC of 2 (mol of O_2) mol^{-1}. Thus, in the next step, the role of large OSC should be evaluated by the catalytic conversion of model reactions, such as CO oxidation.

The present study is focused on evaluating the oxygen release/storage and catalytic properties of Pd-loaded $Pr_2O_2SO_4$ by means of cycled feed stream methods. The dynamic oxygen release/storage characteristics were evaluated quantitatively by a flow microbalance and then correlated with the crystal structural change measured by in situ X-ray diffraction. Anaerobic CO conversion was then tested under cycled feed stream conditions with the aim of evaluating the role of large OSC on catalytic properties. Unlike the automotive processes, the present work used cycled feed streams at very low frequencies to characterize the structure–reaction relationship of a large OSC under unsteady-state conditions.

2. Experimental

2.1. Catalyst preparation

$Pr_2O_2SO_4$ was synthesized via a template route as reported previously [14]. $Pr(NO_3)_3{\cdot}6H_2O$ (8.06 g), $C_{12}H_{25}OSO_3Na$ (SDS) (10.89 g), 28% aqueous NH_3 (37.5 ml), and water (20 ml) were mixed at 40 °C for 1 h to yield a transparent solution and then aged with stirring at 60 °C for more than 10 h. The solution was then cooled to room temperature, with precipitate formation occurring at pH 11. The precipitate thus obtained was collected by centrifugal separation, washed thoroughly with ion-exchanged and distilled water, dried by evacuation at room temperature, and finally heated at 600 °C for 5 h in air. As-calcined $Pr_2O_2SO_4$ was impregnated with an aqueous solution of $Pd(NO_3)_2$ and then calcined at 450 °C for 5 h to produce Pd-loaded samples (1 wt% loading). The as-prepared catalyst exhibited a BET surface area of 18 $m^2\,g^{-1}$ and Pd dispersion of approximately 2%. Pd-loaded catalysts were also prepared using CeO_2-ZrO_2 and γ-Al_2O_3 as reference oxide supports. CeO_2-ZrO_2 was prepared as described previously [8], and γ-Al_2O_3 was supplied from the Catalysis Society of Japan.

2.2. Characterization and reaction

The reduction/reoxidation behavior of the product was measured by a flow microbalance (TG, Rigaku 8120) connected to a controlled gas-supply system. The sample (10 mg) was first heated in a flowing gas mixture of 1.4% H_2 and He (70 $cm^3\,min^{-1}$) at a constant rate (10 °C min^{-1}) up to 900 °C. After the measurement, the sample was cooled to ambient temperature in a stream of 1.4% H_2/He. This was followed by the second heating in a flowing gas mixture of 0.7% O_2/He (20 $cm^3\,min^{-1}$) at the same rate up to 900 °C, to measure the reoxidation profiles.

The structural changes during reduction and reoxidation were measured by in situ X-ray diffraction (XRD), using a Rigaku RINT-Ultima diffractometer (Cu$K\alpha$, 30 kV, 20 mA) equipped with a high-speed, two-dimensional detector (D/teX-25). The sample was placed in a stream of 5% H_2 or 5% O_2 balanced with N_2 (100 $cm^3\,min^{-1}$) in a temperature-controllable chamber, and the XRD pattern was measured at constant intervals of 3 min with a scan rate of 40 deg min^{-1}. Using a high-speed detector enabled rapid scanning of each XRD patterns within 90 s, short enough to neglect phase changes occurring during data acquisition.

Dynamic reduction–oxidation cycles were also measured using the microbalance (Rigaku 8120). First, the sample (10 mg) was heated in a stream of He up to 500–700 °C. On approaching a constant weight at each temperature, the gas feed was switched with programmed time intervals between 1.4% H_2 in He and 0.7% O_2 in He (70 $cm^3\,min^{-1}$) with the sample weight recorded.

Anaerobic CO oxidation under cycled feed stream conditions was conducted at constant reaction temperatures (500–700 °C) in a dual-supply flow system. Two gas feeds, 1% CO/He and 0.5% O_2/He, were alternately switched with programmed time intervals. The rate of gas feed was controlled at $W/F = 4\times10^{-3}$ or 2×10^{-3} g min cm^{-3}. The concentrations of each gas component (CO, CO_2, and O_2) were recorded before and after the catalyst bed using a quadrupole mass spectrometer (Pfeiffer, Omnistar).

3. Results and discussion

3.1. Redox property of Pd-loaded $Pr_2O_2SO_4$

The reduction and reoxidation properties of $Pr_2O_2SO_4$ were first studied by using a flow microbalance. Fig. 1a shows the TG curves of unloaded and 1 wt% Pd-loaded $Pr_2O_2SO_4$ measured in a flow of 1.4% H_2 balanced with He. The reduction of unloaded $Pr_2O_2SO_4$ started at around 600 °C and ended at $\geqslant$800 °C, yielding a weight loss close to 16%, which corresponds to the value calculated assuming the stoichiometric oxygen release from $Pr_2O_2SO_4$ to form Pr_2O_2S. The temperature required for this reduction process could be reduced by loading 1 wt% Pd; that is, the reduction started at 500 °C and was completed at $\leqslant$750 °C, yielding the same weight loss. After measuring the reduction profiles, the sample was cooled to ambient temperature in a flow of 1.4%

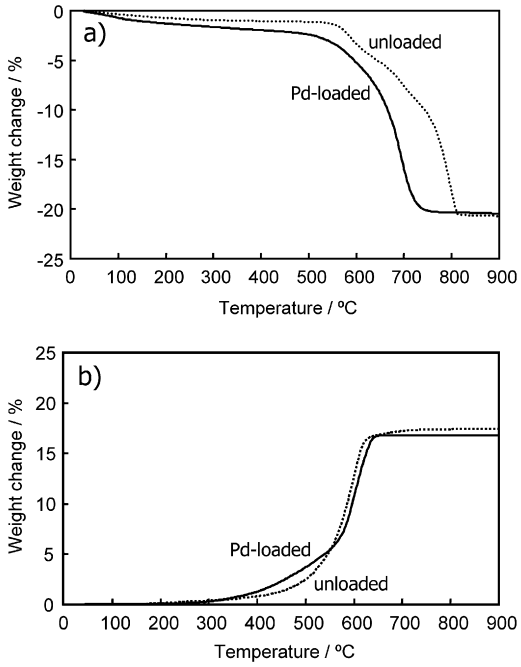

Fig. 1. TG curves of unloaded and 1 wt% Pd-loaded $Pr_2O_2SO_4$ measured (a) in a flow of 1.4% H_2 balanced with He and subsequently, (b) in a flow of 0.7% O_2 balanced with He. Heating rate: 10 °C min^{-1}.

H_2/He, and submitted to second measurement in a flow of 0.7% O_2/He at the same heating rate. Fig. 1b shows the reoxidation profiles thus obtained, where the weight gain started at 400 °C and was completed at 600 °C. The onset of reoxidation was also found to be promoted by loading Pd, but the shift of the TG curve was much smaller compared with that of the reduction profiles shown in Fig. 1a. The total weight gains in both cases were close to the value, 18.5%, calculated assuming stoichiometric oxygen uptake by Pr_2O_2S to form $Pr_2O_2SO_4$.

The phase change during heating in a flow of 5% H_2 could be confirmed by in situ XRD measurement. Fig. 2 exhibits the XRD patterns obtained at 3-min intervals after the gas feed started at 700 °C. In case of unloaded $Pr_2O_2SO_4$ (a), Pr_2O_2S appeared at about 30 min, but the transformation was not completed even after 50 min. In contrast, Pd/$Pr_2O_2SO_4$ began to yield Pr_2O_2S at 20 min, and $Pr_2O_2SO_4$ almost disappeared after 50 min (b). The reduction in both cases was due to direct-phase transformation from $Pr_2O_2SO_4$ to Pr_2O_2S, where no intermediates were observed. Although deposition of Pd metal could not be detected because of the small amount of loading, the reduction of PdO to Pd should take place before the reduction of $Pr_2O_2SO_4$. These results demonstrate the promoting effect of Pd on the reduction of $Pr_2O_2SO_4$ to Pr_2O_2S. According to subsequent in situ XRD measurements at the same temperature in a stream of 5% O_2, in both cases the reoxidation of Pr_2O_2S was completed within 10 min. This is consistent with the weight gain in Fig. 1b being observed at a lower temperature compared with the weight loss in Fig. 1a, where the effect of Pd was less obvious.

Fig. 3 displays the weight changes during dynamic oxygen release/storage cycles of unloaded and 1 wt% Pd-loaded

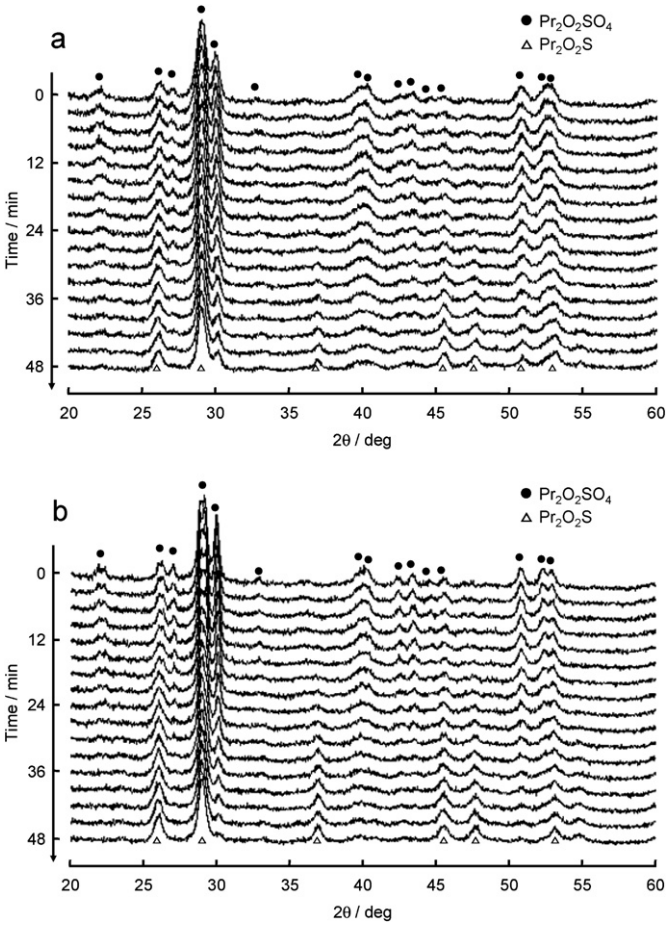

Fig. 2. In situ XRD patterns of (a) unloaded and (b) 1 wt% Pd-loaded $Pr_2O_2SO_4$ measured at 3 min interval at 700 °C in a flow of 5% H_2 balanced with He.

$Pr_2O_2SO_4$ under a cycled feed stream condition (0.7% O_2 or 1.4% H_2) at different temperatures. Unloaded $Pr_2O_2SO_4$ exhibited weight oscillation at 700 °C, with a very small amplitude at the beginning that increased with an increasing number of cycles. Even in the last part of the measurement, however, the amplitude corresponds to <60% of the stoichiometric change between $Pr_2O_2SO_4$ and Pr_2O_2S. A negligible weight change at lower temperatures (⩽600 °C) is consistent with the reduction profile shown in Fig. 1. In contrast, Pd-loaded $Pr_2O_2SO_4$ demonstrated a reversible and stable weight change even at 600 °C, the oscillation amplitude of which corresponds to approximately 85% of the stoichiometric change. The weight changes due to reduction as well as reoxidation were reproducible, but the reduction of Pd/$Pr_2O_2SO_4$ in 1.4% H_2 took more than 1 h, compared with the 5 min required for subsequent reoxidation in 0.7% O_2. From the slope of weight change for each of the system at 700 °C, the apparent rate of reduction, as well as that of reoxidation, can be calculated. The rate of reduction increased from 0.07 to 0.34 (mmol of O_2) g^{-1} min^{-1} by loading 1 wt% Pd, whereas the rate of reoxidation was almost the same, ca. 0.7 (mmol of O_2) g^{-1} min^{-1}. According to our previous study [13], the faster reoxidation compared with reduction is characteristic of the Pr system, because smooth redox between Pr^{3+} and Pr^{4+} on the surface can promote the

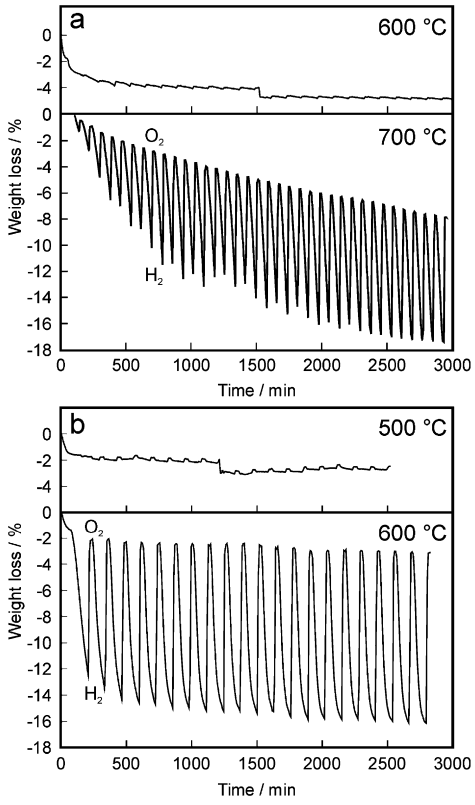

Fig. 3. Weight changes of (a) unloaded $Pr_2O_2SO_4$ and (b) 1 wt% Pd-loaded $Pr_2O_2SO_4$ under cycled feed stream of 0.7% O_2 and 1.4% H_2 at different temperatures.

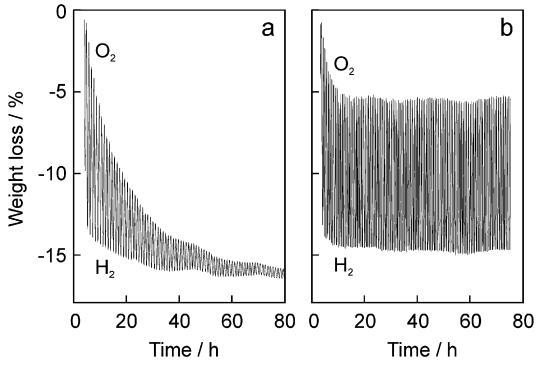

Fig. 4. Weight changes of 1 wt% Pd-loaded $Pr_2O_2SO_4$ under cycled feed stream of 0.7% O_2 and 1.4% H_2 at 800 °C (a) in the absence of SO_2 and (b) in the presence of 30 ppm SO_2.

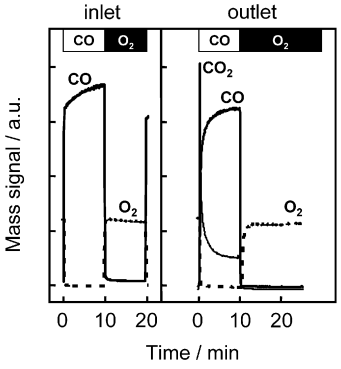

Fig. 5. Effluent gas profiles from 1 wt% Pd/Al_2O_3 under cycled feed stream of 0.5% O_2 and 1% CO at 700 °C. W/F = 4×10^{-3} g min cm^{-3}.

reoxidation of bulk Pr_2O_2S to $Pr_2O_2SO_4$. These two different oxidation states were detected by XPS even after reduction treatment, suggesting that Pr^{3+} can be easily oxidized by air. This is completely different from the other lanthanide oxysulfate; for example, in the $La_2O_2SO_4/La_2O_2S$ system, the reoxidation of La_2O_2S is rather slow compared with the reduction of $La_2O_2SO_4$, because of the poor redox ability of La^{3+}. Due to the redox behavior of Pr^{3+}/Pr^{4+}, gaseous oxygen would be adsorbed as a negatively charged species onto the surface and thus may promote the oxidation of S^{2-} to SO_4^{2-}.

The effect of Pd loading on the reduction of $Pr_2O_2SO_4$ to Pr_2O_2S can be explained by catalytic and/or spillover of hydrogen. It is considered that H_2 first chemisorbs onto impregnated Pd and activated hydrogen species thus formed are supplied to the three-phase boundary among Pd, $Pr_2O_2SO_4$, and the gas phase to cause the reduction to Pr_2O_2S. In addition, spillover of hydrogen from Pd onto the surface of $Pr_2O_2SO_4/Pr_2O_2S$ may accelerate the reduction. It has been suggested that the reduction of several metal oxides is facilitated by spillover hydrogen due to the higher reactivity of atomic hydrogen compared with molecular hydrogen [19].

Owing to the relatively higher temperatures required to the present redox system, phase stability is very important. As we reported previously [12], the Pr oxysulfate does not decompose up to 1000 °C in a static O_2 or H_2 atmosphere. Thus, the sulfur content could be kept almost constant even after several reduction/reoxidation cycles. However, the stability in a long-term dynamic feed stream cycles has not been tested at high temperature. Fig. 4a exhibits weight changes of 1 wt% $Pd/Pr_2O_2SO_4$ during more than 100 redox cycles at 800 °C. The amplitude of weight oscillation was decreased and completely lost after 100 h. Comparing Figs. 3 and 4a clearly shows that the stability decreased drastically at temperatures above 600 °C. The instability is caused by the loss of sulfur due to the decomposition of $Pr_2O_2SO_4$ to the Pr oxide ($Pr_2O_2SO_4 \rightarrow 1/3Pr_6O_{11} + SO_2 + 1/6O_2$). In contrast, stability was improved significantly when 30 ppm SO_2 was supplied in the gas feed (Fig. 4b). This finding can be explained by the shift of the equilibrium to the reverse direction, namely from Pr oxide and SO_2/O_2 to $Pr_2O_2SO_4$. The XRD measurement demonstrated that Pr_6O_{11} after exposure to 30 ppm SO_2 at 800 °C restored the $Pr_2O_2SO_4$ phase.

3.2. Anaerobic CO oxidation over Pd-loaded $Pr_2O_2SO_4$

Next, the Pd-loaded $Pr_2O_2SO_4$ was applied to anaerobic CO oxidation to ensure the effect of large OSC on the catalytic behavior. In this experiment, two gas feeds to a catalyst bed were switched between 1% CO and 0.5% O_2 balanced with He at a constant temperature of 500–700 °C. The reaction was first performed on two reference catalysts, 1 wt% $Pd/\gamma\text{-}Al_2O_3$ and 1 wt% $Pd/CeO_2\text{-}ZrO_2$, before applying to the present 1 wt% $Pd/Pr_2O_2SO_4$ catalyst.

Fig. 5 illustrates the typical gas concentration profiles at inlet as well as outlet of the catalyst bed when 1 wt% $Pd/\gamma\text{-}Al_2O_3$ (surface area, 180 m^2 g^{-1}) was used as a reference catalyst at

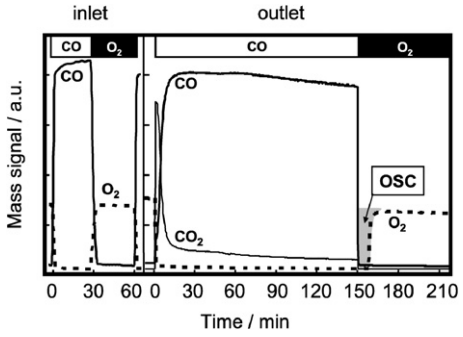

Fig. 6. Effluent gas profiles from 1 wt% Pd/CeO_2-ZrO_2 under cycled feed stream of 0.5% O_2 or 1% CO at 700 °C. W/F = 2×10^{-3} g min cm^{-3}.

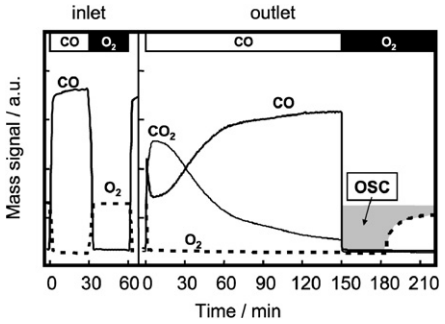

Fig. 7. Effluent gas profiles from 1 wt% Pd/$Pr_2O_2SO_4$ under cycled feed stream of 0.5% O_2 and 1% CO at 700 °C. W/F = 2×10^{-3} g min cm^{-3}.

700 °C. The O_2-to-CO switch yielded a temporal CO_2 peak with simultaneous consumption of CO, presumably suggesting CO oxidation by PdO species. Soon after this, however, CO conversion declined rapidly because of the lack of oxygen release from the catalyst. The subsequent CO-to-O_2 switch gave rise to a very small O_2 uptake due to the oxidation of Pd to PdO. Consequently, the total amount of anaerobic CO oxidation was very low (<10%). When a Pd catalyst supported on the conventional oxygen storage material, CeO_2-ZrO_2 (surface area, 92 $m^2\,g^{-1}$), was used, the conversion of CO to CO_2 was higher after the O_2-to-CO switch (Fig. 6). The initial activity and amount of CO converted were greater than those of Pd/Al_2O_3, because anaerobic CO oxidation was caused by lattice oxygens of CeO_2-ZrO_2. After the CO conversion was almost lost, the gas feed was switched to O_2. Nevertheless, no oxygen was detected in the effluent due to O_2 storage until the breakthrough after about 7 min. The OSC calculated from the oxygen breakthrough curve, 0.8 (mmol of O_2) g^{-1}, was close to the corresponding theoretical capacity of 0.25 (mol of O_2) mol^{-1} and was almost the same with the amounts of CO reacted and CO_2 formed.

Compared with these two reference catalysts, the Pd-loaded $Pr_2O_2SO_4$ exhibited very different concentration profiles, as shown in Fig. 7. It should be noted that a half amount of catalyst is used here, that is, W/F = 2×10^{-3} g min cm^{-3}, compared with W/F = 4×10^{-3} g min cm^{-3} for the reactions shown in Figs. 5 and 8. During CO supply, the conversion to CO_2 was continued for a longer time even in the absence of O_2 in the gas phase. The initial CO conversion was high but decreased gradually, probably because the rate is increasingly determined by

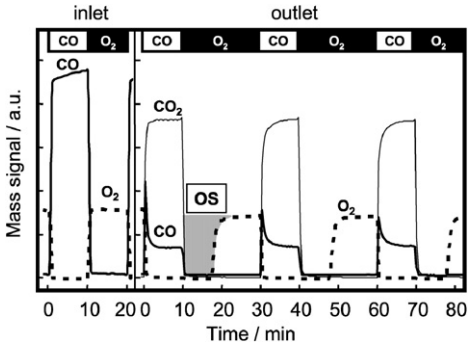

Fig. 8. Effluent gas profiles during CO/O_2 cycle reactions over 1 wt% Pd/$Pr_2O_2SO_4$ under feed stream of 0.5% O_2 or 1% CO at 700 °C. W/F = 4×10^{-3} g min cm^{-3}.

mass transfer in a solid. A subsequent CO-to-O_2 switch caused the O_2 storage. Unlike the Pd/CeO_2-ZrO_2 case (Fig. 6), however, the breakthrough required longer than 30 min. Accordingly, the OSC calculated from the oxygen breakthrough curve achieved a much larger value of 4.6 (mmol of O_2) g^{-1}, in agreement with the theoretical capacity of 2 (mol of O_2) mol^{-1}. The observed OSC and the amount of CO converted (9.2 mmol g^{-1}) are indicative of stoichiometric CO oxidation to CO_2 under the anaerobic condition. When the unloaded $Pr_2O_2SO_4$ was used, the amount of CO converted in a same period (150 min) became very low (ca. 2 mmol g^{-1}), so that oxygen release took longer to complete. This indicates that loading of Pd could provide a number of active site for CO oxidation and thus accelerate the oxygen release from $Pr_2O_2SO_4$. The effluent concentration profile in one cycle corresponds to the full-capacity oxygen release and storage of $Pr_2O_2SO_4$, which could be repeated by applying a cycled feed stream.

Judging from the height of the peak in the effluent CO_2 profiles in Figs. 6 and 7, the initial catalytic activity of Pd/$Pr_2O_2SO_4$ for anaerobic CO oxidation was lower than that of Pr/CeO_2-ZrO_2. The lower activity can be explained by the dispersion of Pd, which was determined by CO adsorption technique to be ca. 10% for CeO_2-ZrO_2 compared with <2% for $Pr_2O_2SO_4$. Thus, the catalytic activity of Pd/$Pr_2O_2SO_4$ can be improved by optimizing the impregnation process of Pd precursors.

Fig. 8 shows the effluent gas profile when the two gas feeds to Pd/$Pr_2O_2SO_4$ were switched repeatedly at 700 °C, with intervals of 10 and 20 min for CO and O_2, respectively. The amount of both CO and O_2 supplied per cycle was 1.1 mmol g^{-1}. Considering the full capacity of oxygen release/storage [4.9 (mmol of O_2) g^{-1}], the interval set here is very short, corresponding to about 20% of full OSC. Therefore, the decay of CO conversion during a step could not be observed. Instead, almost constant CO conversion and oxygen storage could be cycled without deactivation. More than 85% conversion of CO to CO_2 was observed during CO half-cycles, whereas almost half of the O_2 supplied (designated OS in Fig. 8) was stored by the catalyst during O_2 half-cycles. From these profiles, we can calculate the amounts of reacted CO and oxygen storage at each step as a function of reaction temperature as shown in Fig. 9. At 700 °C, the amount of O_2 storage per cycle was 0.49 mmol g^{-1}, which

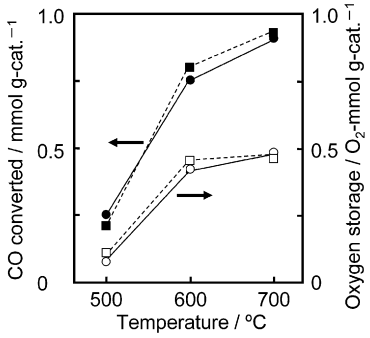

Fig. 9. Temperature dependence of amounts of oxygen storage and CO converted during single CO/O_2 cycle over 1 wt% Pd/$Pr_2O_2SO_4$ as shown in Fig. 8 (●, ○) in the absence of SO_2, (■, □) in the presence of 100 ppm SO_2.

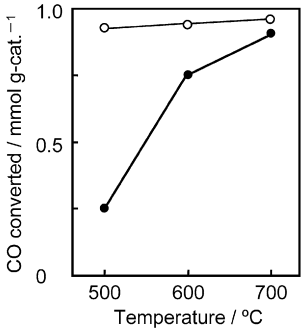

Fig. 10. The amount of CO converted in single CO step (10 min) in Fig. 8 compared with that in corresponding steady-state CO oxidation over 1 wt% Pd/$Pr_2O_2SO_4$. (●) Cycled feed stream, (○) steady-state.

corresponds to about half of the reacted CO, 0.94 mmol g^{-1}; this also suggests the occurrence of stoichiometric anaerobic CO oxidation during each cycles. Both oxygen storage and reacted CO decreased with decreasing reaction temperatures because the reaction rate is determined by mass transfer in the solid, but the ratio of CO converted to O_2 storage remained almost constant, near 2. The CO/O_2 cycled feed stream reactions were also carried out in the presence of 100 ppm SO_2; the amounts of CO reacted and oxygen storage are shown in Fig. 9. Clearly, the activity for CO oxidation and the OSC were not affected by SO_2. Because SO_2 can improve the stability of the redox between oxysulfate and oxysulfide (see Fig. 4b), the present system would be better applied in a sulfur-containing atmosphere.

Fig. 10 exhibits the results of CO/O_2 reaction under the cycled feed stream condition and corresponding steady-state CO oxidation over 1 wt% Pd/$Pr_2O_2SO_4$. The steady-state reaction was carried out by supplying a constant feed stream of 1% CO, 1.5% O_2, and He balance to the catalyst bed at the same W/F of 4×10^{-3} g min cm^{-3}. Here the amount of CO converted in a 10-min period is plotted to allow comparison with that in a single CO step (10 min) of cycled feed stream reaction (Fig. 8). It can be seen that the anaerobic CO oxidation by Pd/$Pr_2O_2SO_4$ is as fast as the steady-state CO-O_2 reaction at sufficiently high temperatures (700 °C). This is a very important feature considering real automotive conditions, in which acceleration and deceleration will leave the catalyst under lean or rich exhausts for a longer time. In such cases, catalysts capable of rapidly releasing or storing a large quantity of O_2 are necessary. Fig. 10 clearly shows that the drawback of the present oxygen storage catalyst is low activity at lower temperatures because of the slow oxygen release compared with the catalytic reactions. Consequently, we are now focusing on improving the low-temperature oxygen storage performance of the present oxysulfate materials by combining with various transition metals and their oxides.

4. Conclusion

The catalytic property of a large-capacity oxygen storage material, $Pr_2O_2SO_4$, was studied under cycled feed stream conditions. Impregnated Pd catalysts accelerated the redox cycles between $Pr_2O_2SO_4$ and Pr_2O_2S, which achieved a large OSC of 2 (mol of O_2) mol^{-1} at $\geqslant$600 °C. The large OSC was found to be useful for the anaerobic oxidation of CO in cycled feed streams at low frequencies. The catalytic activity, as well as OSC, increased with increasing reaction temperature. The rate of CO oxidation was comparable to that of steady-state CO-O_2 reaction at sufficiently high temperatures (700 °C). The effect of SO_2 in the gas feed on catalytic activity was not obvious, but the stability in a long-term reduction/reoxidation cycles at 800 °C could be improved significantly in the presence of SO_2.

Acknowledgments

This study was supported by Industrial Technology Research Grant Program from the New Energy and Industrial Technology Development Organization (NEDO) of Japan and by a Grant-in-Aid for Scientific Research on Priority Area (440) from the Ministry of Education, Culture, Sports, Science and Technology (MEXT).

References

[1] K.C. Taylor, Automobile catalytic converters, in: J.R. Anderson, M. Boudart (Eds.), Catalysis–Science and Technology, vol. 5, Springer-Verlag, Berlin, 1984.
[2] S. Bernal, J. Kaspar, A. Trovarelli, Catal. Today 2 (1999) 50.
[3] A. Trovarelli, in: A. Trovarelli (Ed.), Catalysis by Ceria and Related Materials, vol. 2, Imperial College Press, London, 2002.
[4] M. Ozawa, M.M. Kimura, A. Isogai, J. Alloys Compd. 193 (1993) 73.
[5] F. Zamur, A. Trovarelli, C. de Leitenburg, G. Dolcetti, J. Chem. Soc. Chem. Commun. (1995) 965.
[6] G. Balducci, P. Fornasiero, R. Di Monte, J. Kaspar, S. Meriani, M. Graziani, Catal. Lett. 33 (1995) 193.
[7] J. Kaspar, P. Fornasiero, M. Graziani, Catal. Today 50 (1999) 285.
[8] T. Ohmata, H. Kishimoto, S. Matsumo, N. Ohtori, N. Umesaki, J. Solid State Chem. 147 (1999) 573.
[9] M. Pijolat, M. Prin, M. Soustelle, O. Touret, P. Nortier, J. Chem. Soc. Faraday Trans. 91 (1995) 3941.
[10] N. Kakuta, S. Ikawa, T. Eguchi, K. Murakami, H. Ohkita, T. Mizushima, J. Alloys Compd. 408–412 (2006) 1078.
[11] M. Machida, K. Kawamura, K. Ito, Chem. Commun. (2004) 662.
[12] M. Machida, K. Kawamura, K. Ito, K. Ikeue, Chem. Mater. 17 (2005) 1487.
[13] M. Machida, T. Kawano, M. Eto, D.J. Zhang, K. Ikeue, Chem. Mater. 19 (2007) 954.
[14] M. Machida, K. Kawamura, T. Kawano, D.J. Zhang, K. Ikeue, J. Mater. Chem. 16 (2006) 3084.

[15] M. Boaro, C. de Leitenburg, G. Dolcetti, A. Trovarelli, J. Catal. 193 (2000) 338.
[16] C. Descorme, R. Taha, N. Mouaddib-Mral, D. Duprez, Appl. Catal. A Gen. 223 (2002) 287.
[17] P.S. Lambrou, C.N. Costa, S.Y. Christou, A.M. Efstathiou, Appl. Catal. B Environ. 54 (2004) 237.
[18] X.P. Dai, R.Y. Li, C.C. Yu, Z.P. Hao, J. Phys. Chem. B 110 (2006) 22531.
[19] P.A. Sermon, G.C. Bond, Catal. Rev. 8 (1973) 211.